Effect of the *tert*-butiloxycarbonyl protecting group on the adsorption of protected amino-cyclopentene on the Si(100) surface

Hugo R. R. Santos,[1] Gregori Ujaque,[2] Maria J. Ramos,[1] and José A. N. F. Gomes[1,*]
[1]*REQUIMTE, Departamento de Química, Faculdade de Ciências, Universidade do Porto, Rua do Campo Alegre 687, 4169-007 Porto, Portugal*
[2]*Unitat de Química Física, Departament de Química, Edifici C.n, Universitat Autónoma de Barcelona, 08193 Bellaterra, Catalonia, Spain*
(Received 10 October 2006; published 12 March 2007)

In this work, we study the effects of the *tert*-butiloxycarbonyl protecting group at the adsorption coverage of protected 1-amino-3-cyclopentene (ACP) on the Si(100) surface by using a large cluster with a quantum-mechanical/quantum-mechanical hybrid calculation methodology. We find that at lower coverages, the adsorption energies do not vary significantly from the ones obtained previously for the unprotected ACP form. At medium coverages, we find some energetic deviations that are due to counter-intuitive attractive forces between the adsorbed molecules. These attractive forces make it more probable to find groups of two and three protected ACP (BACP) molecules adsorbed right next to each other. Higher surface coverages, however, seem to be severely affected by geometrical restrictions that should be enough to prevent further adsorption. In the end, we conclude that the protecting group works extremely well and can actually increase the final attainable coverage for ACP on the Si(100) surface.

DOI: 10.1103/PhysRevB.75.125413 PACS number(s): 68.43.Bc, 68.43.Fg, 68.47.Fg

I. INTRODUCTION

In 2002 Lin *et al.*[1] used the 1-amino-3-cyclopentene (ACP) molecule to functionalize the Si(100) surface as a first step in a process that aimed to attach single-stranded DNA (ssDNA) to the same surface for later use as a specific DNA sensor. Problems encountered in the efficiency of their method[2–8] have made them use the *tert*-butyloxicarbonyl (tBOC) group to protect the amino group of the ACP molecule to prevent it from reacting with the Si(100) surface. The protected ACP (BACP) was found to have a much better behavior when connecting to the surface. When it was later on deprotected and all the remaining surface preparation steps were executed, it was found that it would lead to a correctly functionalized surface. When this surface was then used as a ssDNA sensor, it was found that it could be used to detect even single-base mismatches between the tester ssDNA attached to the surface and the complementary ssDNA in the tested solution. These tests, however, showed that continuous use of this surface for ssDNA sensing resulted in a decrease of the measured optical signal with each testing cycle, i.e., the sensor showed that it was not stable or robust enough to allow for continuous use.[1] However, similar studies performed in carbon surfaces[9] showed that the signal stays relatively stable in time, and this makes us wonder if the problem is not in the different protection requisites of each of these surfaces. Silicon surfaces are prone to oxidizing attack,[10] while carbon surfaces are much more resilient.

The tBOC protecting group seems to function correctly because its volume is keeping away the amino group from the surface.[11] This is exactly what it was supposed to do, but then another problem arises. Is the tBOC group avoiding a large portion of the surface to be covered by the functionalization process? Is it inducing a large portion of holes in the functionalization layer? These can be important issues since they can compromise surface protection against oxidizing agents[10] such as water[12] and oxygen[13] present in the DNA samples that will have to be subsequently analyzed by the sensor. In this work, we tried to address these problems and understand how the protecting group is affecting the final coverage of the surface.

Some previous theoretical work has been done on the adsorption of ACP on the Si(100) surface.[11,14–16] It was shown that the ACP maximum coverage could ideally achieve roughly half-monolayer (0.5 ML) coverage.[16] This is in agreement with scanning tunneling microscopy studies done with cyclopentene,[17,18] which show that this molecule typically adsorbs in half-monolayer coverages on the Si(100) surface. Since the amino group is small and its position in the molecule upon adsorption is not affecting the apparent surface area occupied by each ACP molecule when compared with cyclopentene, we would expect them to behave similarly. However, when we start thinking about the tBOC protecting group, we quickly realize that its volume can indeed present a problem and induce a lower surface functionalization coverage. Since the protecting group is later on removed, this would leave a lower quality functionalization, with the surface full of holes. Ideally, we would want complete surface coverage,[19–21] but that is not possible even with the unprotected ACP, so we were expecting that the maximum attainable coverage for the protected form would be similar to the unprotected one.[14] With this work, we tried to find some answers to this problem by testing different adsorption patterns on the surface. Basically, we tested several combinations of adsorbed molecules and free surface spots and observed how they affect the adsorption energies relative to their positions and distances.

II. METHODOLOGY

In this work, we used the same methodology that we had previously used when studying the unprotected ACP cover-

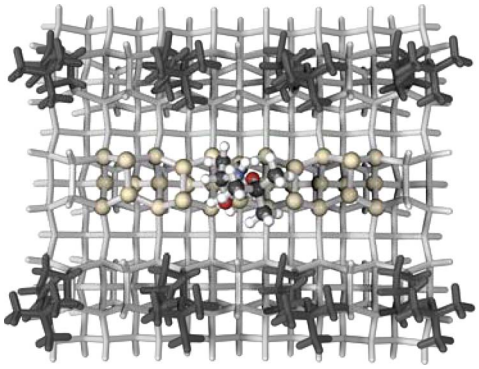

FIG. 1. (Color online) Top view of the $Si_{273}H_{104}$ cluster. Balls represent the higher-level layer atoms and sticks represent the lower-level layer ones. Light gray sticks represent silicon atoms and dark gray sticks represent BACP atoms.

age on the Si(100) surface,[14] i.e., we used a large cluster ($Si_{273}H_{104}$) and a quantum-mechanical/quantum-mechanical hybrid calculation scheme (ONIOM),[22–24] as implemented in the Gaussian03 software package.[25] We concentrated the higher-level density-functional theory[26–28] (DFT) methodology (B3LYP) (Ref. 29) with the SHC* basis set[30,31] in the central part of the cluster, where the adsorption is made, and the lower-level semiempirical AM1 method[32] in the outer part. With this cluster, we can easily represent 21 surface dimers, disposed in a 7×3 array, reserving the central five dimers as the testing positions for our study. These five central dimers are the ones represented by the high-level DFT method, while the remaining 16 outer dimers are accounted for by the AM1 calculation and serve as a constant, controllable and more realistic environment for the central part.[33]

In the five central positions, we tested several coverage situations by using different combinations of occupied and unoccupied dimers. The dimers where BACP adsorption occurred are the occupied positions, while the free and clean silicon dimers are the unoccupied ones. By calculating the differences between different combinations, we could understand the effect that the environment surrounding an adsorbing BACP molecule could induce on its adsorption energy. The cluster's lower-level outer part has been made invariable throughout all the calculation structures and represents a 0.5 ML coverage; that is, from the 16 dimers present in this situation, half of the positions are occupied with adsorbed BACP molecules, while the free dimers have been kept passivated with hydrogen atoms. Figure 1 shows a top view of the cluster with a single BACP molecule adsorbed in the central testing position and the eight lower layer BACP molecules that emulate the 0.5 ML coverage represented in dark gray sticks.

To represent the different combinations, we devised a symbolic representation consisting of a sequence of five *A* or "_" to represent an occupied or an unoccupied position, respectively. In this formalism, a representation of *AAAAA* denotes a fully covered surface, that is, a complete monolayer (1 ML), while a representation of _ _*A*_ _ symbolizes a single adsorbed BACP molecule in the central position (as shown on Fig. 1). The *A*_*A*_*A* and _*A*_*A*_ representations both, refer, to a half-monolayer coverage (0.5 ML).

In a previous work where we studied the coverage effects on the unprotected ACP molecule,[14] we started by calculating the fully covered surface structure and then proceeded by removing molecules from the surface to get the desired coverages. In this work, however, we did it the other way around, starting with the clean surface and then binding molecules to it to get the desired coverages. This was done for two reasons. First, when we tried calculating the fully covered surface model, we found that the BACP molecules were very mobile and interfered with each other much more than the ACP molecules. That meant that the optimizations were more difficult and took more CPU time to perform. Second, since we know that the surface coverage should be no higher than the one that we found for the unprotected ACP (approximately 0.5 ML), it made no sense to spend that amount of calculation time and resources to perform those big calculations right from the beginning. This fact affects the comparison between ACP and BACP, since we do not have exactly the same structures. Even so, we can easily compare similar situations and take valid conclusions from it.

III. RESULTS AND DISCUSSION

It should be noted that all the calculated values refer to adsorption electronic potential energies and not to adsorption free energies. This means that no temperature or entropic effects are being taken into account. The reason for that is that the calculations are too big for us to be able to calculate those corrections. However, since we are mainly doing a comparative study, the absolute values are not very important given that these corrections should not be too different in all the calculations. The relative values should be, on the whole, barely affected. Moreover, a previous theoretical study[11] has calculated these corrections for the adsorption of ACP on Si(100) and found that they accounted for 10–12 kcal mol^{-1}. Therefore, we can simply assume that these corrections should be roughly the same and take that value into account when we see the values presented in this work.

A. Single-molecule adsorption energy variation

Since we had five testing positions in the cluster, we had to check if all of them were equivalent. Ideally, they should be exactly the same with the possibility to find a small difference when the adsorbed molecule was aligned or not with the molecules present in the outer lower-level part. For instance, Fig. 1 shows a situation where the central adsorbed molecule is not aligned with any of the lateral row molecules. If it was adsorbed one position to the left or to the right, then it would be aligned.

The results for the five single-molecule adsorptions are presented in Table I. We can clearly see that there is a tendency for higher (more negative) adsorption energies in the extremes of the testing positions, where we found values around −42 kcal mol^{-1}, and gradually decreasing in a more or less symmetric way to the central position, where we found a value of −39.5 kcal mol^{-1}. We do not see a pattern indicating alignment with the molecules adsorbed in the lateral dimer rows. This result shows us two things. First, there

TABLE I. Single BACP molecule adsorption energies. **A** represents the adsorbing molecule.

Transition	ΔE (kcal mol^{-1})
_____ → ____**A**	−42.2
_____ → ___**A**_	−40.4
_____ → __**A**__	−39.5
_____ → _**A**___	−41.2
_____ → **A**____	−42.0

is no significant repulsion between molecules adsorbed in adjacent dimer rows; i.e., although the protecting groups are bulky, the distance between silicon rows is large enough to easily accommodate them. Second, our cluster model is showing some weakness in the representation of the adsorbed structures at the limits of the testing zones. This clearly happens because the DFT cluster part has a limited size, and although the semiempirical part is avoiding a representation where the DFT part ends directly into vacuum, it is still not enough to completely eliminate that effect. This also means that all the calculations performed in small cluster models should be affected by this variation, which, in our case, even using an outer layer, accounts for nearly 3 kcal mol^{-1}. To avoid this variation, we should only compare structures where the molecules are adsorbing in the same position, which, ideally, should be the central one.

B. 0.5 ML adsorption states

Table II shows several final structures where the adsorbing molecule is two positions away from another molecule already present at the surface; i.e., there is always a free silicon dimer in between. We can see that the adsorption values for different positions and neighborhoods barely change from the comparable single-molecule adsorption structures. At most, we see a decrease of a few tenths of kcal mol^{-1} This means that, as we had seen for the ACP molecule, the BACP molecules can easily adsorb in a 0.5 ML coverage without feeling any repulsive effects between them. In fact, by comparing the last two values in Table II, we can see that there seems to be a slight stabilization effect between molecules, since we observe that adding another molecule at two positions away from the adsorbing one actually increases the adsorption energy in 0.3 kcal mol^{-1}. This

TABLE II. 0.5 ML coverage BACP molecule adsorption energies. **A** represents the adsorbing molecule.

Transition	ΔE (kcal mol^{-1})
_*A*___ → _*A*_**A**_	−40.1
___*A*_ → _**A**_*A*_	−40.9
_*AA*__ → _*AA*_**A**	−42.7
__*A*__ → __*A*_**A**	−41.9
____*A* → __**A**_*A*	−39.2
*A*___*A* → *A*_**A**_*A*	−39.5

TABLE III. Adsorption energies for the formation of two- and three-molecule BACP molecule groups. **A** represents the adsorbing molecule.

Transition	ΔE (kcal mol^{-1})
__*A*__ → __*A***A**_	−35.1
___*A*_ → __**A***A*_	−36.1
_*A*___ → _*A***A**__	−36.4
__*A*__ → _**A***A*__	−37.4
_*AA*__ → _*AA***A**_	−30.5
_*A*_*A*_ → _*A***A***A*_	−26.0
_*AA*__ → _**A***AA*_	−30.5

same situation can be seen in the third structure, which shows a difference of 0.8 kcal mol^{-1} to the next structure and is 0.5 kcal mol^{-1} higher than the equivalent single-molecule adsorbed structure. Although this effect is small, it is still relevant and it looks like it is caused by an attractive force between adjacent adsorbed molecules, most probably interactions between the NH and the COO groups of the protecting groups. The possibility of formation of hydrogen bonds involving these groups is discussed in Sec. III D.

C. Higher coverage structures

Next, we tried to understand how the molecules would behave if they adsorbed right next to each other, creating groups of two or three molecules in consecutive dimers in the same dimer row. Table III shows the structures used to understand this. On the whole, what can be seen is that the energies are not as low as we would expect them to be. Although these bulky molecules are adsorbing right next to each other, the difference between the equivalent single-molecule adsorption is roughly 4 kcal mol^{-1} for the two-molecule groups and 10–14 kcal mol^{-1} for the three-molecule groups. This happens for two reasons. First, the adsorbed molecules have relatively high flexibility in their connection to the surface. This allows them to bend and get farther away from each other, providing the space needed. However, this also happened with the unprotected ACP form, and we still did not see these small energy differences. The second reason explains this, since we can now clearly notice that there is a significant effect resulting from attractive forces that are stabilizing these molecules that get close at the surface and, obviously, the closer the molecules get the more significant this effect turns out to be.

Figure 2 shows a side view of the central dimer row of the cluster representing the _*AAA*_ structure. We can clearly see that the BACP molecules are bent relative to the surface to provide space for each other. Furthermore, the distortion is such that further adsorption right next to this three-molecule group should be very hard to accomplish.

D. Hydrogen-bond formation

The introduction of a carboxylic group in the system has some significance. The coexistence of C═O groups right

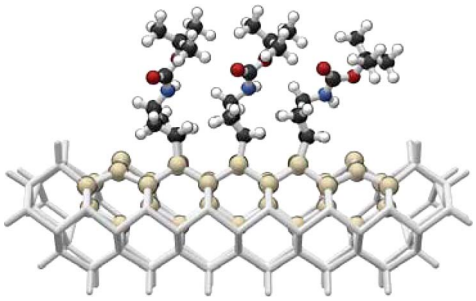

FIG. 2. (Color online) Side view of the central dimer row of the cluster showing the *_AAA_* structure. Balls represent the high layer atoms and sticks represent the low layer ones.

next to N—H groups always represents the possibility of formation of hydrogen bonds between adjacent molecules. Indeed, we found that formation of hydrogen bonds is possible in this system when two molecules adsorb right next to each other. However, this is accomplished at the expense of some energy that is being used to distort the molecules, so that they align in such a way that the relevant groups come closer. We found that the adsorption energy for the H-bond-containing structures was actually lower (less negative) than that of the equivalent structures with no H bond by 3 kcal mol^{-1}; i.e., the energy required to overcome the distortion and repulsion that allow the molecules to form the H bond is actually higher than the stabilization energy that results from its formation. Figure 3 shows the side view of two *_AA__* structures with the upper one showing the optimized geometry for the structure with no hydrogen bond and the lower one showing the structure containing the hydrogen bond. The large geometrical distortion required for H-bond formation is clearly visible. The distance between the oxygen atom and the nitrogen of the amino group involved in the H

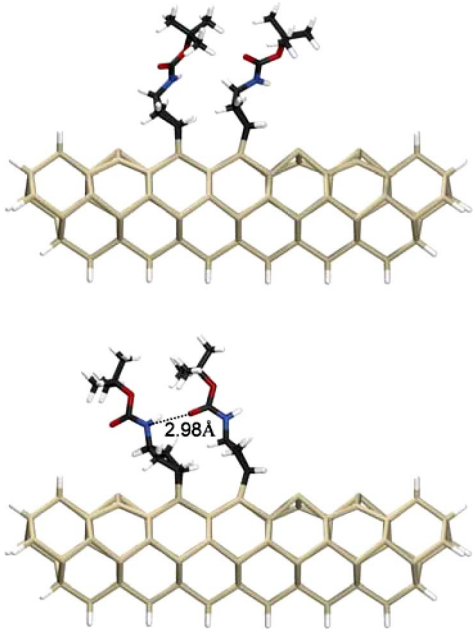

FIG. 3. (Color online) Side view of the *_AA_*-structures without formation of H bond (top) and with H bond (bottom).

TABLE IV. Adsorption energy comparison between equivalent BACP and ACP structures. **A** represents the adsorbing molecule.

	ΔE (kcal mol^{-1})	
Structure	BACP	ACP
*__***A**__	−39.5	−39.3
*A_***A**_*A*	−39.5	−38.5
*_A***A**__	−36.4	−34.5
*_A***A***A*_	−25.6	−19.5

bond (O···H—N) is 2.98 Å, while the oxygen to hydrogen distance (O···H) is 2.04 Å. The $\hat{OHN}$ angle is 151°. All of these values are quite typical for a hydrogen bond.

E. BACP vs ACP comparison

To understand exactly what are the differences that result from the use of the protecting group, we show in Table IV the comparison between equivalent situations for the protected and unprotected ACP forms. To minimize energy variation from the cluster model as discussed above, we are only comparing structures where the adsorbing molecule is always in the central position. What can be seen is that, on the whole, the same tendency is found for both molecules. However, the BACP energies decline less steeply than the ACP ones with increasing surface coverage. When we get to the three-molecule groups, we can see that the difference already accounts for 6 kcal mol^{-1} As previously discussed, this is a result of the attractive interactions between adjacent molecules and may be responsible for higher than 0.5 ML coverage surfaces. There is, however, no experimental study that has ever addressed this issue, so we can only put forward the hypothesis. Even taking into account the entropic and temperature corrections, we would still get an adsorption energy of roughly −13 kcal mol^{-1}, which is quite significant. However, the problem that the creation of these groups may face is a kinetic one and not a thermodynamic one. The adsorption process for these molecules must involve the formation of the intermediate state, which may be severely affected by the lack of space when approaching the surface. Since this intermediate state is not very stable with an adsorption energy of around −7 kcal mol^{-1},[12] any obstructions can have a significant effect. Our work, however, cannot address this issue, and only a reaction path study can give a definitive answer to this question.

IV. CONCLUSION

In this paper, we showed that the tBOC protecting group used to avoid adsorption through the amino group to the Si(100) surface when adsorbing ACP does work as expected without creating a worse coverage scenario than the equivalent unprotected form would do. The space left between adsorbed molecules at a half-monolayer coverage is enough to provide space for the bulky protecting group. Moreover, we found out that the adsorption group, due to an increase in the

attractive forces between the adsorbing molecules, actually slightly improves the energy of the higher coverage structures when compared to the unprotected forms. This should make it more probable to find groups of two and three adsorbed molecules in consecutive dimers on the surface. We do not know, however, if these structures are created at a reasonable speed or if the kinetics of the process is highly affected due to possible constraints in the formation of the required transition state. This answer can only be obtained through reaction path calculations or desorption scans, which we have not yet performed.

We also found that our cluster model, although big, still suffers from limited size problems. We saw that the five central positions (out of seven in the same row and 21 on the whole cluster) were not equivalent, showing energetic variation of almost 3 kcal mol^{-1} This should be taken into account when adsorption studies are performed in small cluster models and total energies are being calculated.

ACKNOWLEDGMENTS

H.R.R.S. thankfully acknowledges the Fundacão para a Ciência e Tecnologia (FCT) for the Ph.D. grant reference SFRH/BD/21401/2005, access to the Centres de Computació i Comunicacions de Catalunya (CEPBA-CESCA), and funding through the HPC-Europa's Transnational Access Program, project (RII3-CT-2003-506079), with the support of the European Community-Research Infrastructure Action of the FP6. G.U. acknowledges the Spanish MEC for funding through the CTQ2005-09000-C02-01 project and the "Ramon y Cajal" program.

*Corresponding author. Electronic address: jfgomes@fc.up.pt

[1] Z. Lin, T. Strother, W. Cai, X. Cao, L. M. Smith, and R. J. Hamers, Langmuir **18**, 788 (2002).
[2] J. S. Hovis, H. Liu, and R. J. Hamers, J. Phys. Chem. B **102**, 6873 (1998).
[3] M. A. Filler and S. F. Bent, Prog. Surf. Sci. **73**, 1 (2003).
[4] T. Vo-Dinh, J. P. Alarie, N. Isola, D. Landis, A. L. Wintenberg, and M. N. Ericson, Anal. Chem. **71**, 358 (1999).
[5] J. Janata, Analyst (Cambridge, U.K.) **119**, 2275 (1994).
[6] F. Bozso and P. Avouris, Phys. Rev. Lett. **57**, 1185 (1986).
[7] X. Cao and R. J. Hamers, J. Vac. Sci. Technol. B **20**, 1614 (2002).
[8] J.-H. Cho and L. Kleinman, Phys. Rev. B **67**, 201301(R) (2003).
[9] W. Yang, O. Auciello, J. E. Butler, W. Cai, J. A. Carlisle, J. E. Gerbi, D. M. Gruen, T. Knickerbocker, T. L. Lasseter, J. John, N. Russell, L. M. Smith, and R. J. Hamers, Nat. Mater. **1**, 253 (2002).
[10] J. Dabrowski and H.-J. Müssig, *Silicon Surfaces and Formation of Interfaces* (World Scientific, Singapore, 2000).
[11] H. R. R. Santos, M. J. Ramos, and J. A. N. F. Gomes, Phys. Rev. B **72**, 075445 (2005).
[12] P. A. Thiel and T. E. Madey, Surf. Sci. Rep. **7**, 211 (1987).
[13] T. Engel, Surf. Sci. Rep. **18**, 93 (1993).
[14] G. Festa, M. Cossi, V. Barone, G. Cantele, D. Ninno, and G. Iadonisi, J. Chem. Phys. **122**, 184714 (2005).
[15] G. Cantele, F. Trani, D. Ninno, M. Cossi, and V. Barone, J. Phys.: Condens. Matter **18**, 2349 (2006).
[16] H. R. R. Santos, G. Ujaque, M. J. Ramos, and J. A. N. F. Gomes, J. Comput. Chem. **27**, 1892 (2006).
[17] J. S. Hovis, H. Liu, and R. J. Hamers, Appl. Phys. A: Mater. Sci. Process. **66**, S553 (1998).
[18] R. J. Hamers, J. S. Hovis, C. M. Greenlief, and D. F. Padowitz, Jpn. J. Appl. Phys., Part 1 **38**, 3879 (1999).
[19] N. K. Chaki and K. Vijayamohanan, Biosens. Bioelectron. **17**, 1 (2002).
[20] W. Senaratne, L. Andruzzi, and C. K. Ober, Biomacromolecules **6**, 2427 (2005).
[21] S. Onclin, B. J. Ravoo, and D. N. Reinhoudt, Angew. Chem. **44**, 6282 (2005).
[22] F. Maseras and K. Morokuma, J. Comput. Chem. **16**, 1170 (1995).
[23] S. Dapprich, I. Komáromi, K. S. Byun, K. Morokuma, and M. J. Frisch, J. Mol. Struct. **461**, 1 (1999).
[24] K. Morokuma and T. Vreven, J. Comput. Chem. **21**, 1419 (2000).
[25] M. J. Frisch, G. W. Trucks, H. B. Schlegel, G. E. Scuseria, M. A. Robb, J. R. Cheeseman, J. Montgomery, J. A., T. Vreven, K. N. Kudin, J. C. Burant, J. M. Millam, S. S. Iyengar, J. Tomasi, V. Barone, B. Mennucci, M. Cossi, G. Scalmani, N. Rega, G. A. Petersson, H. Nakatsuji, M. Hada, M. Ehara, K. Toyota, R. Fukuda, J. Hasegawa, M. Ishida, T. Nakajima, Y. Honda, O. Kitao, H. Nakai, M. Klene, X. Li, J. E. Knox, H. P. Hratchian, J. B. Cross, V. Bakken, C. Adamo, J. Jaramillo, R. Gomperts, R. E. Stratmann, O. Yazyev, A. J. Austin, R. Cammi, C. Pomelli, J. W. Ochterski, P. Y. Ayala, K. Morokuma, G. A. Voth, P. Salvador, J. J. Dannenberg, V. G. Zakrzewski, S. Dapprich, A. D. Daniels, M. C. Strain, O. Farkas, D. K. Malick, A. D. Rabuck, K. Raghavachari, J. B. Foresman, J. V. Ortiz, Q. Cui, A. G. Baboul, S. Clifford, J. Cioslowski, B. B. Stefanov, G. Liu, A. Liashenko, P. Piskorz, I. Komaromi, R. L. Martin, D. J. Fox, T. Keith, M. A. Al-Laham, C. Y. Peng, A. Nanayakkara, M. Challacombe, P. M. W. Gill, B. Johnson, W. Chen, M. W. Wong, C. Gonzalez, and J. A. Pople, GAUSSIAN 03, Revision C.02, Gaussian Inc., Wallingford, CT, 2004.
[26] P. Hohenberg and W. Kohn, Phys. Rev. **136**, B864 (1964).
[27] W. Kohn and L. J. Sham, Phys. Rev. **140**, A1133 (1965).
[28] R. G. Parr and W. Yang, *Density-Functional Theory of Atoms and Molecules* (Oxford University Press, Oxford, 1989).
[29] A. D. Becke, J. Chem. Phys. **98**, 5648 (1993).
[30] T. H. Dunning, Jr. and P. J. Hay, *Modern Theoretical Chemistry* (Plenum, New York, 1977).
[31] A. K. Rappé, T. A. Smedley, and W. A. Goddard III, J. Phys. Chem. **85**, 1662 (1981).
[32] M. J. S. Dewar, E. G. Zoebisch, E. F. Healy, and J. J. P. Stewart, J. Am. Chem. Soc. **107**, 3902 (1985).
[33] H. R. R. Santos, M. J. Ramos, and J. A. N. F. Gomes, C. R. Chim. **8**, 1461 (2005).